Mammalian Alanine/Glyoxylate Aminotransferase 1 Is Imported into Peroxisomes via the PTS1 Translocation Pathway. Increased Degeneracy and Context Specificity of the Mammalian PTS1 Motif and Implications for the Peroxisome-to-Mitochondrion Mistargeting of AGT in Primary Hyperoxaluria Type 1

Alison Motley,* Michael J. Lumb,‡ Paru B. Oatey,‡ Patricia R. Jennings,‡ Priyal A. De Zoysa,‡ Ronald J. A. Wanders,§ Henk F. Tabak,* and Christopher J. Danpure‡

*Department of Biochemistry, E. C. Slater Institute, University of Amsterdam, 1105 AZ Amsterdam, The Netherlands;‡MRC Protein Translocation Group, Department of Biology, and MRC Laboratory for Molecular Cell Biology, University College London, London WC1E 6BT, United Kingdom;§Department of Pediatrics, University of Amsterdam, 1105 AZ Amsterdam, The Netherlands

Abstract. Alanine/glyoxylate aminotransferase 1 (AGT) is peroxisomal in most normal humans, but in some patients with the hereditary disease primary hyperoxaluria type 1 (PH1), AGT is mislocalized to the mitochondria. In an attempt to identify the sequences in AGT that mediate its targeting to peroxisomes, and to determine the mechanism by which AGT is mistargeted in PH1, we have studied the intracellular compartmentalization of various normal and mutant AGT polypeptides in normal human fibroblasts and cell lines with selective deficiencies of peroxisomal protein import, using immunofluorescence microscopy after intranuclear microinjection of AGT expression plasmids. The results show that AGT is imported into peroxisomes via the peroxisomal targeting sequence type 1 (PTS1) translocation pathway. Although the COOH-terminal KKL of human AGT was shown to be necessary for its peroxisomal import, this tripeptide was unable to direct the peroxisomal import of the bona fide peroxisomal protein firefly luciferase or the reporter protein bacterial chloramphenicol acetyltransferase. An ill-defined region immediately upstream of the COOH-terminal KKL was also found to be necessary for the peroxisomal import of AGT, but again this region was found to be insufficient to direct the peroxisomal import of chloramphenicol acetyltransferase. Substitution of the COOH-terminal KKL of human AGT by the COOH-terminal tripeptides found in the AGTs of other mammalian species (SQL, NKL), the prototypical PTS1 (SKL), or the glycosomal PTS1 (SSL) also allowed peroxisomal targeting, showing that the allowable PTS1 motif in AGT is considerably more degenerate than, or at least very different from, that acceptable in luciferase. AGT possessing the two amino acid substitutions responsible for its mistargeting in PH1 (i.e., Pro11→Leu and Gly170→Arg) was targeted mainly to the mitochondria. However, AGTs possessing each amino acid substitution on its own were targeted normally to the peroxisomes. This suggests that Gly170→Arg-mediated increased functional efficiency of the otherwise weak mitochondrial targeting sequence (generated by the Pro11→Leu polymorphism) is not due to interference with the peroxisomal targeting or import of AGT.

Under the putative influence of dietary selection pressure, the intracellular compartmentalization of alanine/glyoxylate aminotransferase 1 (AGT)[1] has changed on many occasions during the evolution of mammals (7, 10). In some mammals, such as rabbits and most humans, AGT is exclusively peroxisomal (3, 7, 27, 45); in other mammals, such as cats and dogs, AGT is mainly mitochondrial (7, 31); in yet other mammals, such as marmosets and rats, AGT is more evenly distributed between both organelles (7, 26, 28, 44). This variable dual compartmentalization of AGT is related to its putative

Drs. Motley and Lumb should be considered as joint first authors of this paper.

Address correspondence to Dr. C. J. Danpure, MRC Laboratory for Molecular Cell Biology, University College London, Gower Street, London WC1E 6BT, United Kingdom. Tel.: 44 171 380 7936. E-mail: c.danpure@ucl.ac.uk

1. *Abbreviations used in this paper*: AGT, alanine/glyoxylate aminotransferase 1; CAT, chloramphenicol acetyltransferase; MTS, mitochondrial targeting sequence; PH1, primary hyperoxaluria type 1; PTS, peroxisomal targeting sequence.

dual metabolic role of glyoxylate detoxification (in the peroxisomes) and gluconeogenesis (in the mitochondria) (7, 10). The functional importance of correct AGT compartmentalization is vividly demonstrated by the human autosomal recessive disorder primary hyperoxaluria type 1 (PH1) (5). In some patients, disease is caused by an unparalleled inter-organelle mistargeting phenomenon in which AGT is aberrantly targeted and imported into the mitochondria (6), where it is unable to fulfil its proper metabolic role of glyoxylate detoxification even though it remains catalytically active.

In all animals studied so far (i.e., human, marmoset, rabbit, rat, cat), AGT is encoded by a single gene (21, 23, 29, 36, 37). Therefore, this gene must have the potential to encode mitochondrial and/or peroxisomal targeting sequences, depending on the particular species. Where present (i.e. in the marmoset, rat, and cat), the cleavable NH_2-terminal mitochondrial targeting sequence (MTS) of AGT has been clearly identified (21, 30, 37). However, the location and nature of the peroxisomal targeting sequence (PTS) of AGT has not been determined.

Acquisition and loss of the ability to target AGT to a particular organelle during mammalian evolution is due to a combination of the use of multiple transcription and translation initiation sites, so that the MTS is either included or excluded from the open reading frame (21, 29, 37, 42). The mistargeting of AGT from the peroxisomes to the mitochondria in some PH1 patients is due to the combined effects of a normally occurring Pro11→Leu polymorphism and a PH1-specific Gly170→Arg point mutation (or possibly a Phe152→Ile mutation in a few patients) (8, 34, 35). The Pro11→Leu polymorphism leads to the generation of a novel, functionally rather weak, noncleavable, NH_2-terminal MTS, that is not homologous with the ancestral MTS (i.e., that found in the marmoset, rat, and cat). It has been suggested previously that the Gly170→Arg and Phe152→Ile mutations, which occur within an internal very highly conserved region of 58 amino acids, might increase the functional efficiency of the otherwise rather weak MTS by inhibiting the peroxisomal targeting and/or import of AGT (34, 35).

In mammals, two types of PTS have been identified so far (39). The first PTS characterized (PTS1) consists of a simple COOH-terminal tripeptide with a consensus sequence of S(A,C)-K(R,H)-L(M) (15, 41). This PTS1 motif, which is not cleaved after import, is found in many mammalian and nonmammalian peroxisomal matrix proteins. SKL has been found not only to be necessary for the import of the model peroxisomal protein firefly luciferase, but also to be sufficient to target otherwise cytosolic proteins (e.g., bacterial chloramphenicol acetyltransferase, CAT) to mammalian peroxisomes when attached to their COOH termini (14, 15).

The only other well-characterized PTS in mammals is the PTS2, which has so far only been clearly identified in 3-ketoacyl-CoA-thiolase. It consists of a cleavable NH_2-terminal sequence of 26 or 36 amino acids depending on species (32, 40) with a putative consensus motif of x_n-RL-x_5-H/QL-x_n, the R and the H being residues −24 and −17, respectively, relative to the presequence cleavage site (11).

The PTS of AGT has yet to be identified. Although there are a number of similarities between the COOH termini of mammalian AGTs (i.e., KKL, SQL, NKL) and recognized PTS1s, and between the NH_2 terminus of at least human AGT (i.e., x_4-KL-x_5-KA-x_n) and recognized PTS2s, neither fulfils the requirements of either a PTS1 or PTS2 mammalian consensus sequence. The identification of two mutations (Gly170→Arg and Phe152→Ile) in a highly conserved internal region of AGT in PH1 patients in whom AGT is mistargeted to the mitochondria has raised the possibility that AGT might contain a novel, internal PTS (4).

In the present study, we have identified the peroxisomal import pathway of AGT and partially characterized the nature of its PTS. In addition, we have further examined the role of the Gly170→Arg mutation in AGT mistargeting. Our results show that AGT is imported via the PTS1 protein translocation machinery. However, the COOH-terminal tripeptide of AGT is shown to be both more context-specific and yet more degenerate than previously found for mammalian PTS1s. In addition, we show that, contrary to previous suggestions, the PH1-specific Gly170→Arg mutation does not interfere with the peroxisomal targeting or import of AGT.

Materials and Methods

AGT and CAT Expression Plasmids

The vector used for the expression of mammalian AGT and bacterial CAT and their various constructs was derived from pHYK (33), which was a kind gift from H. R. B. Pelham (MRC Laboratory of Molecular Biology, Cambridge, UK). pHYK contained the adenovirus major late promoter, the chick lysozyme-coding sequence followed by a c-*myc* epitope and the peptide SEKDEL, the herpes virus *tk* gene polyadenylation site and the SV-40 origin of replication (see Fig. 1 *A*). For the AGT and CAT expression studies, the insert (i.e., lysozyme, the c-*myc* epitope and part of the SEKDEL peptide) between the HindIII and BamHI sites was replaced by the gene construct of interest (see below).

Normal and Mutant PH1 Human AGT Clones and Their Derivatives

The eight plasmids containing normal and mutant PH1 human AGT constructs (pAGT-pgi, pAGT-lgi, pAGT-lri, pAGT-lgm, pAGT-lrm, pAGT-pri, pAGT-prm, and pAGT-pgm) (see Table I) were made by cutting out the inserts of the equivalent clones in pBluescriptKS+ (i.e., pPGI, pLGI, pLRI, pLGM, pLRM, pPRI, pPRM, and pPGM, respectively) (34) with HindIII and BamHI and cloning them into HindIII/BamHI-digested pHYK (see Fig. 1 *A*).

Mutagenesis of the 3′ Terminus of AGT

Human AGT cDNA possesses a single ApaI site (118 bp from the end of the coding region) as does the polylinker of pBluescriptIIKS+. To help with the COOH-terminal PCR mutagenesis strategy (see below), the ApaI site in the pBluescriptIIKS+ was deleted by digesting with ApaI, blunt-ending with T_4 DNA polymerase and religating with T_4 DNA ligase to produce pBS^{ApaI-}. The insert from pPGI (see above) was cut out with HindIII and BamHI and was recloned into HindIII/BamHI-digested pBS^{ApaI-} to produce pBS^{ApaI-}PGI.

$pAGT^{\alpha}$-SKL, $pAGT^{\alpha}$-SQL, $pAGT^{\alpha}$-NKL, $pAGT^{\alpha}$-SSL, $pAGT^{\alpha}$-SEL, $pAGT^{\alpha}$-DEL, and $pAGT^{\alpha}$-LLL (see Table I) were made by amplifying the 3′ end of the insert of pPGI (see above) by PCR, using the primer pairs P9/P2, P9/P5, P9/P4, P9/P3, P9/P6, P9/P8, and P9/P7, respectively (see Table II). The PCR products were digested with ApaI (that cuts 324 bp downstream of P9) and BamHI (cuts within the reverse strand mutagenic primers) and cloned into ApaI/BamHI-digested pBS^{ApaI}-PGI. To check for PCR incorporation errors, the sequences of the inserts were checked between the ApaI and BamHI sites. The inserts were cut out with HindIII and BamHI and recloned into HindIII/BamHI-digested pHYK to

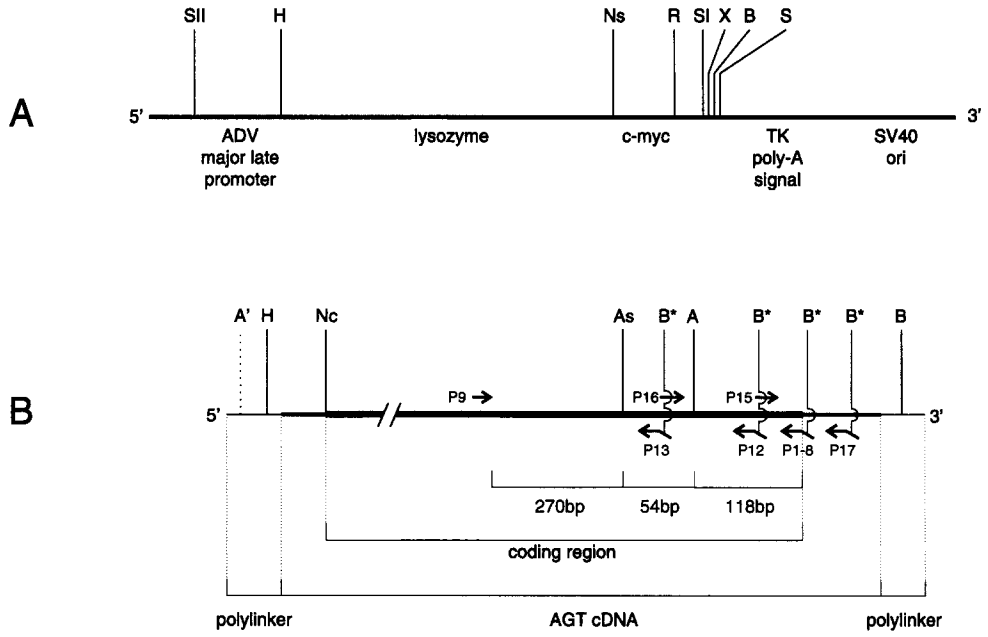

Figure 1. Partial structure of the pHYK expression plasmid (*A*) and PCR strategy for generation of AGT constructs (*B*). Restriction sites: *H*, HindIII; *B*, BamHI (*B**, BamHI sites introduced by −strand primers); *A*, ApaI (*A'*, ApaI site deleted in pBSApaI-); *As*, AspI; *Ns*, NsiI; *X*, XbaI; *R*, EcoRI; *S*, SmaI; *SI*, SacI; *SII*, SacII; *Nc*, NcoI. P1-8, P12, P13, and P17 are −strand primers, and P9, P15, and P16 are (+)strand primers described in Table II.

produce pAGT$^{\alpha}$-SKL, pAGT$^{\alpha}$-SQL, pAGT$^{\alpha}$-NKL, pAGT$^{\alpha}$-SSL, pAGT$^{\alpha}$-SEL, pAGT$^{\alpha}$-DEL, and pAGT$^{\alpha}$-LLL.

pAGT$^{\alpha}$-Δ1 was made as follows. The 3′ portion of the insert of pPGI (see above) was amplified by PCR using the primer pair P9/P1 (see Table II). pPGI and the P9/P1 PCR product were digested separately with ApaI, mixed together and ligated with T_4 DNA ligase. The ligated mixture was then double digested with HindIII and BamHI and the required fragment of ~1.3 kb was gel purified. This was then ligated to the gel-purified large HindIII/BamHI fragment of pBS^{ApaI-} to produce pBS^{ApaI-}AGT$^{\alpha}$-Δ1. The sequence of the PCR amplified portion (i.e., between the ApaI and BamHI sites) was checked for artefacts and then the insert was cut out with HindIII and BamHI and recloned into HindIII/BamHI-digested pHYK to produce pBS^{ApaI-}AGT$^{\alpha}$-Δ1.

pAGT$^{\beta}$-Δ1 was made by digesting pLGM (see above) with NcoI and

Table I. Description of the AGT, CAT, and Luciferase Expression Plasmids Used in the Present Study

Plasmid	Synonym	Description
pAGT-pgi	pAGT$^{\alpha}$	Normal human AGT encoded by the major allele
pAGT-lgi		pAGT$^{\alpha}$ containing a Pro11→Leu substitution
pAGT-1ri		pAGT$^{\alpha}$ containing Pro11→Leu and Gly170→Arg substitutions
pAGT-lgm	pAGT$^{\beta}$	Normal human AGT encoded by the minor allele, containingPro11→Leu and Ile340→Met substitutions
pAGT-lrm	pAGT$^{\gamma}$	Mutant human AGT encoded by the PH1 mistargeting allele, containing Pro11→Leu, Gly170→Arg and Ile340→Met substitutions
pAGT-pri		pAGT$^{\alpha}$ containing a Gly170→Arg substitution
pAGT-prm		pAGT$^{\alpha}$ containing Gly170→Arg and Ile 340→Met substitutions
pAGT-pgm		pAGT$^{\alpha}$ containing a Ile340→Met substitution
pAGT$^{\alpha}$-SKL		COOH-terminal KKL of pAGT$^{\alpha}$ substituted by SKL
pAGT$^{\alpha}$-SQL		COOH-terminal KKL of pAGT$^{\alpha}$ substituted by SQL
pAGT$^{\alpha}$-NKL		COOH-terminal KKL of pAGT$^{\alpha}$ substituted by NKL
pAGT$^{\alpha}$-SSL		COOH-terminal KKL of pAGT$^{\alpha}$ substituted by SSL
pAGT$^{\alpha}$-SEL		COOH-terminal KKL of pAGT$^{\alpha}$ substituted by SEL
pAGT$^{\alpha}$-DEL		COOH-terminal KKL of pAGT$^{\alpha}$ substituted by DEL
pAGT$^{\alpha}$-LLL		COOH-terminal KKL of pAGT$^{\alpha}$ substituted by LLL
pAGT$^{\alpha}$-Δ1		COOH-terminal KKL of pAGT$^{\alpha}$ deleted
pAGT$^{\beta}$-Δ1		COOH-terminal KKL of pAGT$^{\beta}$ deleted
pAGT$^{\alpha}$-Δ2		10 amino acids from −13 to −4, inclusive, deleted from pAGT$^{\alpha}$, the COOH-terminal KKL being kept intact
pAGT$^{\alpha}$-Δ3		44 amino acids from −47 to −4, inclusive, deleted from pAGT$^{\alpha}$, the COOH-terminal KKL being kept intact
pFFL-SKL		Normal firefly luciferase
pFFL-KKL		COOH-terminal SKL of pFFL-SKL substituted by KKL
pCAT		Bacterial chloramphenicol acetyltransferase
pCAT-SKL		SKL added to COOH terminus of pCAT
pCAT-KKL		KKL added to COOH terminus of pCAT
pCAT+AGT13		COOH-terminal 13 amino acids of AGT added to the COOH terminus of pCAT
pCAT+AGT47		COOH-terminal 47 amino acids of AGT added to the COOH terminus of pCAT
pCAT+AGT47-SKL		COOH-terminal KKL of pCAT+AGT47 substituted by SKL

The AGT and CAT plasmids are all based on the parent mammalian expression vector pHYK (see Materials and Methods). The equivalent pBluescriptIIKS+ plasmids are referred to as appropriate in the text. COOH-terminal amino acid substitutions are indicated in upper case (e.g., SKL), whereas internal substitutions are indicated in lower case (e.g., lrm). The luciferase expression plasmids are described in the text.

Table II. Description of Oligonucleotide Primers Used for the Generation of the AGT and CAT Constructs

Primer	Sequence	Maps to:*	Strand	Constructs
P1	5′-AAGAGCTCGGATCCTCACTTGGGGCAGTGCTG-3′	−13 to −27	(−)	pAGT$^{\alpha}$-Δ1
P2	5′-CATCATGGATCCTCACAGCTTCGACTTGGGGCAG-3′	−1 to −22	(−)	pAGT$^{\alpha}$-SKL
P3	5′-CATCATGGATCCTCACAGGCTCGACTTGGGGCAG-3′	−1 to −22	(−)	pAGT$^{\alpha}$-SSL
P4	5′-CATCATGGATCCTCACAGCTTGTTCTTGGGGCAG-3′	−1 to −22	(−)	pAGT$^{\alpha}$-NKL
P5	5′-CATCATGGATCCTCACAGCTGCGACTTGGGGCAG-3′	−1 to −22	(−)	pAGT$^{\alpha}$-SQL
P6	5′-CATCATGGATCCTCACAGCTCCGACTTGGGGCAG-3′	−1 to −22	(−)	pAGT$^{\alpha}$-SEL
P7	5′-CATCATGGATCCTCACAGCAGCAGCTTGGGGCAG-3′	−1 to −22	(−)	pAGT$^{\alpha}$-LLL
P8	5′-CATCATGGATCCTCACAGCTCGTCCTTGGGGCAG-3′	−1 to −22	(−)	pAGT$^{\alpha}$-DEL
P9	5′-CTTCTCCTTCTCCCTGGACA-3′	−469 to −450	(+)	All pAGT constructs
P10	5′-CATCATGGATCCTTATAATTTTGACGCCC-3′	+9 to −8	(−)	pCAT-SKL
P11	5′-CATCATGGATCCTTATAATTTTTTCGCCC-3′	+9 to −8	(−)	pCAT-KKL
P12	5′-CGTCGTGGATCCTCACAGCTTCTTGGCCTCCGTCACGCG-3′	−43 to −57	(−)	pAGT$^{\alpha}$-Δ2
P13	5′-CGTCGTGGATCCTCACAGCTTCTTAATGTCGAAGTGGTC-3′	−145 to −159	(−)	pAGT$^{\alpha}$-Δ3
P14	5′-CATCATGGATCCCATGCATGCGCCCCGCCCTGCCACTC-3′	−4 to −21	(−)	pFCAT
P15	5′-CTGAGGGCGGCCCTGCAGC-3′	−42 to −24	(+)	pCAT+AGT(13)
P16	5′-GAGATCATGGGTGGCCTTG-3′	−144 to −126	(+)	pCAT+AGT(47)
P17	5′-GTTTGCTCCGGATCCCTCAG-3′	+72 to +53	(−)	pCAT+AGT(13)

P1-8 are − strand PCR primers used for modifying the COOH terminus of AGT. P1, P2, P3, P4, P5, P6, P7, and P8 were used to generate pAGT$^{\alpha}$-Δ1, pAGT$^{\alpha}$-SKL, pAGT$^{\alpha}$-SSL, pAGT$^{\alpha}$-NKL, pAGT$^{\alpha}$-SQL, pAGT$^{\alpha}$-SEL, pAGT$^{\alpha}$-LLL, and pAGT$^{\alpha}$-DEL, respectively. P12 and P13 are − strand primers used for making the internal AGT deletion constructs pAGT$^{\alpha}$-Δ2 and pAGT$^{\alpha}$-Δ3. P9 is the + strand primer used in combination with P1-8, P12, and P13. P10 and P11 are − strand PCR primers used for making the COOH-terminal pCAT-SKL and pCAT-KKL fusions, respectively. P14 is a − strand primer used to make the general purpose CAT fusion vector pFCAT. P10, P11, and P14 were used in conjunction with the M13 reverse sequencing primer as the + strand primer. P15 and P16 are + strand primers used with the − strand primers P17 and M13 universal sequencing primer, respectively, to make the CAT-AGT fusions pCAT+AGT13 and pCAT+AGT47. Bold type indicates the parts of the primers that hybridise to the starting AGT or CAT templates, the nonbold type indicating the non-hybridising 5′ tails. The single underlines indicate the BamHI (and SphI in the case of P14) restriction sites used for cloning. The double underlines indicate the mutant bases. *, The nucleotides to which the primers (hybridizing sequences) map are numbered from the last base of the original stop codon (i.e. base −1). P1-9, P12, P13, and P15-17 map to AGT sequences and P10, P11, and P14 map to CAT sequences. P17 maps to the 3′UTR of AGT, whereas all other primers (except the M13 primers) map to coding regions.

ApaI and cloning the 1.2-kb fragment into NcoI/ApaI-digested pBS^{ApaI}-AGT$^{\alpha}$-Δ1. This was then digested with HindIII and BamHI and the insert cloned into HindIII/BamHI-digested pHYK.

Two AGT constructs, pAGT$^{\alpha}$-Δ2 and pAGT$^{\alpha}$-Δ3, in which the 10 or 44 amino acids immediately upstream of the COOH-terminal KKL (i.e., residues −13 to −4 or −47 to −4 inclusive) were deleted (see Table I), were made as follows. pPGI was amplified by PCR using primer pairs P9/P12 or P9/P13, respectively (see Table II). The products were cut with AspI (cuts 270 bp downstream of P9, see Fig. 1 *B*) and BamHI (cuts in the reverse-strand primers), and cloned into AspI/BamHI-digested pBS^{ApaI}-PGI. After checking for possible PCR errors between the AspI and BamHI sites, the HindIII/BamHI fragments of these constructs were then cloned into HindIII/BamHI-digested pHYK to produce pAGT$^{\alpha}$-Δ2 and pAGT$^{\alpha}$-Δ3.

Generation of the COOH-terminal CAT Fusions

The insert of pBLCAT2 (20), comprising the coding region of the CAT gene together with the T intron and polyadenylation signal, was cut out with BglII and SmaI. The BglII site was blunt-ended with DNA polymerase I (Klenow fragment) and the product was cloned into the EcoRV site of pBluescriptIIKS+. A positively orientated clone was selected (pBSCAT) and the HindIII/BamHI-digested insert was cloned into the HindIII and BamHI sites of pHYK to make pCAT. pCAT-SKL (see Table I) was made by amplifying the insert of pBSCAT by PCR, using the M13 reverse sequencing primer (+ strand) and the mutagenic primer P10 (− strand) (Table II). The PCR product was cut with NcoI (cuts within the CAT coding region) and BamHI (cuts within P10) and the NcoI/BamHI fragment was cloned back into pBSCAT, replacing the native fragment, to produce pBSCAT-SKL. After checking for PCR errors between the NcoI and BamHI sites, the HindIII/BamHI fragment of pBSCAT-SKL was cloned into HindIII/BamHI-digested pHYK to produce pCAT-SKL. pCAT-KKL (see Table I) was produced similarly, except that the PCR template was pBSCAT-SKL and the mutagenic primer was P11 (Table II).

To simplify the construction of larger CAT-AGT fusions, a general purpose CAT-fusion vector pFCAT was made as follows. pBSCAT was amplified by PCR using primer P14 (Table II) and the M13 reverse sequencing primer. P14 places a SphI site across the final codon of CAT that, after digestion and incubation with T_4 DNA polymerase, creates a blunt end immediately after the final codon. The PCR product was digested with NcoI (cuts 142 bp upstream of the end of the coding region) and BamHI (cuts in P14 downstream of the SphI site) and cloned back into pBSCAT digested with NcoI and BamHI (cuts in the polylinker). The sequence between the NcoI and BamHI sites was checked for PCR artefacts.

Two COOH-terminal CAT-fusions, pCAT+AGT13 and pCAT+AGT47 (see Table I), which included the last 13 or 47 amino acids of AGT, respectively, were made as follows. pPGI was amplified by PCR using primer pairs P15/P17 or P16/M13 universal primer, respectively (see Table II). The products were blunt-ended with T_4 DNA polymerase, digested with BamHI (cuts downstream of the AGT stop codon in P17 when the latter was used or in the polylinker when the M13 primer was used), and cloned into pFCAT, which had previously been digested with SphI, blunt-ended with T_4 DNA polymerase, and then digested with BamHI. After checking for possible PCR artefacts between the COOH terminus of CAT and the AGT stop codon, the resulting in-frame fusions were digested with HindIII and BamHI and cloned into HindIII/BamHI-digested pHYK to produce pCAT+AGT13 and pCAT+AGT47. pCAT+AGT47-SKL was made by replacing the ApaI/BamHI fragment of pCAT+AGT47 with the equivalent fragment of pAGT$^{\alpha}$-SKL.

Firefly Luciferase Expression Plasmids and Mutagenesis of the 3′ Terminus of Firefly Luciferase

Construction of the plasmid expressing normal firefly luciferase (pFFL-SKL) has been described previously (referred to as pCDNALuc in reference 24). pFFL-KKL was made by amplifying by PCR the insert of pFFL-SKL using the T_7 (+strand) primer and the COOH-terminal (− strand) mutagenic primer 5′-TTTTCTGCAGTTACAATTTTTTCTTTCCGC-CCTTCTTGGCC-3′ that contained a PstI restriction site (*underlined*). The resulting 1.8-kb PCR fragment was digested with PstI and BamHI (cuts in the 5′ polylinker) and cloned into the BamHI/PstI-digested parent expression vector pCDNA (24). The 1.5-kb BamHI/EcoRV fragment was replaced by the corresponding fragment from pFFL-SKL and the sequence of the remaining 0.3-kb PCR-amplified portion (between the EcoRV and PstI sites) was checked for artefacts.

Cell Culture and Human Fibroblast Cell Lines

Primary skin fibroblasts were used for microinjection experiments and were derived either from control subjects (cell lines 85AD5035F, HENG90AD, and MC98) or from two patients suffering from peroxisome assembly disorders: the PTS1$^-$ line was derived from a neonatal adrenoleukodystrophy patient (cell line AAL85AD) and the PTS2$^-$ line was de-

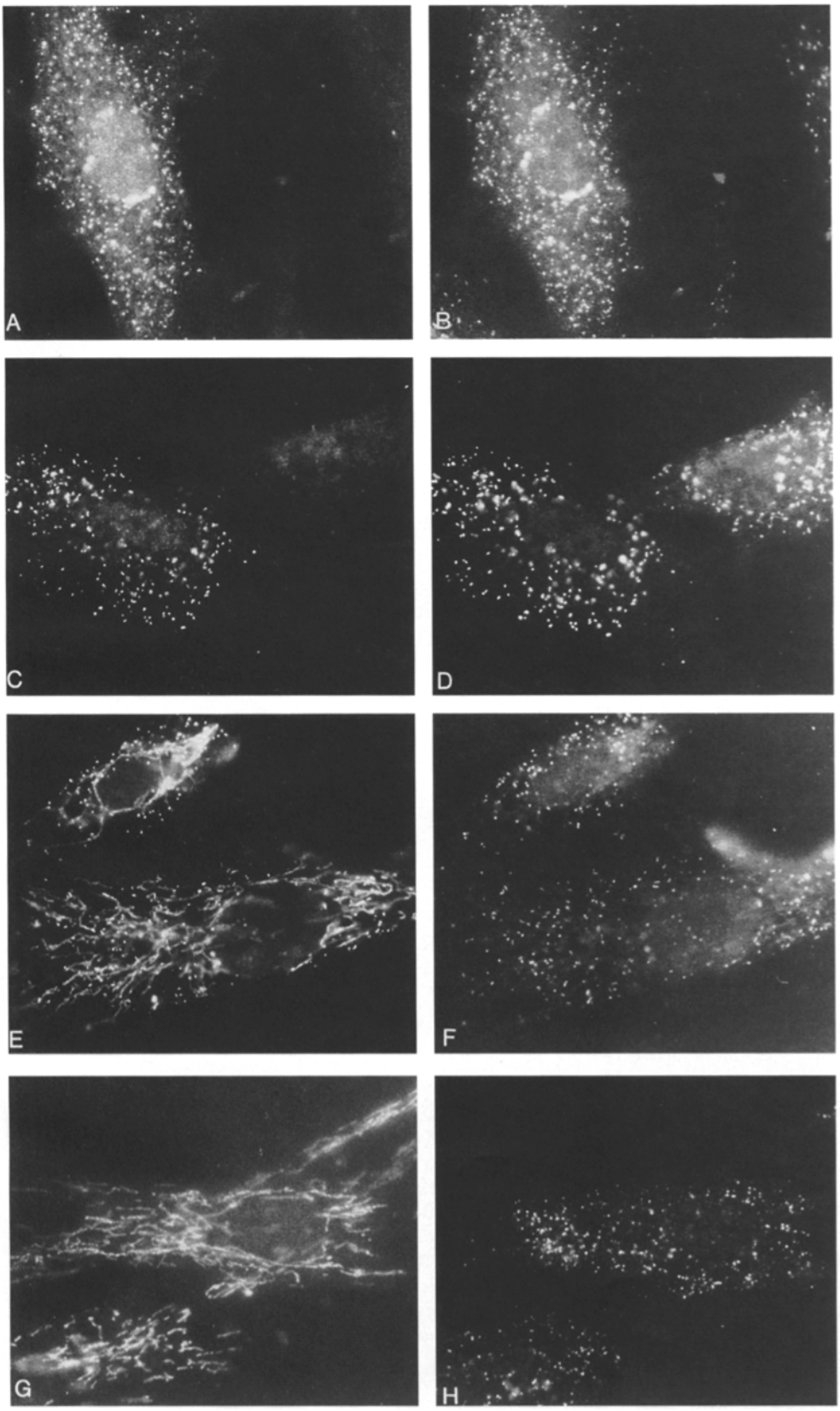

Figure 2. Intracellular localization of naturally occurring normal and PH1 AGTs in normal human fibroblasts. Double-label immunofluorescence of AGT^{α} (*A*), AGT^{β} (*C*), and AGT^{γ} (*E*) and peroxisomal thiolase (*B*, *D*, and *F*, respectively). Double-labeling patterns in normal human fibroblasts of an endogenous mitochondrial protein (cytochrome oxidase [*G*]) and a peroxisomal protein (thiolase [*H*]) are shown for comparison.

rived from a patient suffering from rhizomelic chondrodysplasia punctata (cell line MCHE85AD). These cell lines have been characterized in detail elsewhere (24). Cells were grown in a 1:1 mixture of Dulbecco's modified Eagle's medium and Ham's F10 (GIBCO BRL, Glasgow, UK) supplemented with 10% fetal calf serum (GIBCO BRL) under 5% CO_2. Cells were split 1:4 on reaching confluence and were not used above passage 30.

Microinjection

24 h before microinjection, the cells were plated onto microinjection grids or cover slips. The needles were made using a PB-7 micropipette puller (Narishage Co., Tokyo, Japan) and DNA was injected in reverse PBS (4 mM Na_2HPO_4, 1 mM KH_2PO_4, 140 mM KCl, pH 7.3). DNA was injected

at a concentration of 0.05 mg/ml, equivalent to ~50 molecules per injection. Except where indicated in the text, 18 h after microinjection, the cells were processed for immunofluorescence microscopy.

Immunofluorescence Microscopy

The cells were washed in PBS and fixed in freshly prepared 4% (wt/vol) paraformaldehyde/0.1% Triton X-100 (pH 7.5) for 20 min at room temperature. For differential permeabilization, the cells were fixed in 4% paraformaldehyde in PBS for 20 min and treated with 25 μg/ml digitonin in PBS (to permeabilize the plasma membrane only) or 25 μg/ml digitonin in PBS, containing 0.1% Triton X-100 (to permeabilize both the plasma membrane and the peroxisomal membrane). Free aldehyde groups were blocked by incubating for 10 min in 0.1 M NH_4Cl in PBS. The cells were then processed for single- or double-label indirect immunofluorescence using the following antibodies: monoclonal mouse anti-rat thiolase (3G4) (17); monoclonal mouse anti-human catalase (43); polyclonal guinea pig anti-rat catalase (kind gift from Dr. S.Yokota, Yamanashi Medical College, Japan); polyclonal guinea pig anti-firefly luciferase (18); polyclonal rabbit anti-bovine cytochrome oxidase (kind gift from Dr. C. van den Bogert, E. C. Slater Institute, Amsterdam); polyclonal rabbit anti-CAT; and polyclonal rabbit anti-human AGT. For the double-labeling experiments, AGT was visualized with FITC- or TRITC-conjugated donkey anti-rabbit IgG (Jackson ImmunoResearch Laboratories, West Grove, PA); firefly luciferase was visualized using FITC-conjugated goat anti-guinea pig IgG (Jackson ImmunoResearch Laboratories); CAT was visualized with FITC-conjugated goat anti-rabbit IgG (Sigma Chemical Co., Poole, UK); and thiolase and catalase were visualized using cy3-conjugated goat anti-mouse IgG (Jackson ImmunoResearch Laboratories) or biotinylated sheep anti-mouse IgG (Amersham International, Amersham, UK) followed by streptavidin-labeled FITC or TRITC (Amersham International). In the CAT double-labeling experiments, catalase was visualized with biotinylated goat anti-guinea pig IgG (Vector Laboratories, Peterborough, UK) followed by avidin-labeled Texas Red (Vector Laboratories). For single labeling, FITC-conjugated donkey anti-rabbit IgG was used. The incubations were all performed at room temperature for 45 min in PBS containing 10 mg/ml BSA (to reduce nonspecific binding). After each incubation the cells were washed extensively in PBS. The injection grids/cover slips were mounted on cover slips/slides, respectively, in either carbonate-buffered glycerol containing p-phenylenediamine or Mowiol (Harlow Chemical Co. Ltd., Harlow, UK) containing DABCO (Sigma Chemical Co.). In most experiments, the fluorescent staining pattern was viewed in an Olympus IMT2 (RFL) fluorescence microscope, using an IMT2DMB filter for excitation of the FITC signal, and an IMT2-DMG filter for excitation of the TRITC signal. FITC fluorescence was visualized in combination with the G520 barrier filter and TRITC fluorescence in combination with the R610 barrier filter. Fluorescent images were recorded on Kodak TMAX 400 ASA B/W film. In the experiments involving the expression of CAT-fusions and internal AGT deletions, the fluorescent staining pattern was viewed in a Biorad MRC1000 confocal laser-scanning microscope, using OG515 (fluorescein) and 585EFLP (tetramethylrhodamine/Texas Red) filters. The captured images were manipulated using Adobe Photoshop software installed on a Macintosh computer, and recorded onto Kodak TMAX 100 ASA B/W film using a Sapphire slide recorder (Management Graphics Inc., Minneapolis, MN).

Results

The subcellular distribution of various naturally occurring and artificial AGT derivatives was determined by immunofluorescence microscopy 18 h after the intranuclear microinjection of AGT expression plasmids. This procedure allowed prolonged expression of the gene of interest, and gave the cells time to recover from the trauma of microinjection before AGT localization was determined.

Compartmentalization of Normal and Mutant PH1 AGT in Normal Human Fibroblasts

Normal human AGTs encoded by both the more common major and less common minor alleles (AGT^{α} and AGT^{β}, respectively) were imported into a particulate compartment which labeled for the peroxisomal marker enzyme 3-ketoacyl-CoA-thiolase in normal human fibroblasts (Fig. 2, *A–D*). No significant mitochondrial localization was detected, even for AGT^{β} that in normal human liver is found to a level of ~5–10% in the mitochondria (in individuals homozygous for the minor AGT allele) (34). On the other hand, the mutant form of AGT found in PH1 patients with the peroxisome-to-mitochondrion AGT mistargeting phenotype (i.e., AGT^{γ}) was localized mainly in the mitochondria with much less in the peroxisomes (Fig. 2, *E* and *F*). This compares with a 90% mitochondrial and 10% peroxisomal localization in livers of PH1 patients who are homozygous for the AGT^{γ} allele (see Table III) (6, 34).

Table III. Summary of the Results for the Intracellular Compartmentalization of Various AGT, Luciferase, and CAT Constructs in Human Fibroblasts Compared with the Distribution of the Endogenous Gene Products (AGT only) in Human Livers

	Subcellular distribution				
	Fibroblasts			Liver	
Plasmid	Normal	PTS1⁻	PTS2⁻	Normal or PH1	Peroxisome assembly disorders
pAGT-pgi ($pAGT^{\alpha}$)	P	C	P	P	C
pAGT-lgi	P	–	–	–	–
pAGT-lri	M + P	–	–	–	–
pAGT-lgm ($pAGT^{\beta}$)	P	C	–	M + P	M + C
pAGT-lrm ($pAGT^{\gamma}$)	M + P	M	–	M + P	–
pAGT-pri	P	C	–	–	–
pAGT-prm	P	–	–	–	–
pAGT-pgm	P	–	–	–	–
$pAGT^{\alpha}$-SKL	P	–	–	–	–
$pAGT^{\alpha}$-SQL	P	–	–	–	–
$pAGT^{\alpha}$-NKL	P	–	–	–	–
$pAGT^{\alpha}$-SSL	P	–	–	–	–
$pAGT^{\alpha}$-SEL	C	–	–	–	–
$pAGT^{\alpha}$-DEL	C	–	–	–	–
$pAGT^{\alpha}$-LLL	C	–	–	–	–
$pAGT^{\alpha}$-Δ1	C	C	–	–	–
$pAGT^{\beta}$-Δ1	C	C	–	–	–
$pAGT^{\alpha}$-Δ2	C	–	–	–	–
$pAGT^{\alpha}$-Δ3	C	–	–	–	–
pFFL-SKL	P	C	P	–	–
pFFL-KKL	C	–	–	–	–
pCAT	C	–	–	–	–
pCAT-SKL	P	–	–	–	–
pCAT-KKL	C	–	–	–	–
pCAT+AGT13	C	–	–	–	–
pCAT+AGT47	C	–	–	–	–
pCAT+AGT47-SKL	P	–	–	–	–

The normal, PTS1⁻ and PTS2⁻ fibroblasts (24) are described in the text. The subcellular distribution in normal liver (3, 34) and peroxisome-assembly disorder liver (9) applies to AGT^{α} and AGT^{β}, while that for PH1 liver (6) applies only to AGT^{γ}. The subcellular distribution is defined as *M* (mitochondrial), *P* (peroxisomal), or *C* (cytosolic). In the cases of endogenous AGT expression, the approximate relative proportions are indicated by the size of the character used. A dash means either that the experiment was not done or that the question is not applicable.

Role of the Gly170→Arg Mutation in the Peroxisome-to-Mitochondrion Mistargeting of AGT in PH1

AGT^{β} contains two amino acid differences compared to AGT^{α} (i.e., Pro11→Leu and Ile340→Met substitutions, see Table I and reference 34). AGT^{γ} contains an addi-

tional Gly170→Arg substitution compared to AGT$^{\beta}$. To determine the roles of these substitutions in the peroxisomal or mitochondrial compartmentalization of AGT, artificial AGT constructs containing all of the possible combinations of the three amino acid differences were expressed in normal fibroblasts (Fig. 3, *A–C*). It was found that only when the Pro11→Leu and Gly170→Arg substitutions were present together (i.e., in AGT-lri, Fig. 3 *B*) was AGT distributed similarly to that found with AGT$^{\gamma}$ (Fig. 2 *E*) (i.e., mitochondrial and peroxisomal). In all other cases, AGT was localized normally in the peroxisomes (Fig. 3, *A* and *C*, summarized in Table III). Most significantly, AGT-pri was peroxisomal (as judged by its colocalization with thiolase, Fig. 3, *C* and *D*), a finding that was surprising as had previously been suggested that the PH1-specific Gly170→Arg mutation might contribute to the peroxisome-to-mitochondria mistargeting phenomenon by interfering with the peroxisomal targeting and/or import of AGT (34, 35).

To determine whether AGT-pri (and in fact AGT$^{\alpha}$) had actually entered the peroxisomal interior and had not just attached to the cytoplasmic face of the organelle, cells expressing AGT-pri (and AGT$^{\alpha}$) were permeabilized differentially. After selective permeabilization of the plasma membrane with low concentrations of digitonin (see reference 24), only a diffuse background labeling could be detected for AGT with no evidence of any punctate distribution (Fig. 3 *E*). However, after permeabilization of both plasma membrane and peroxisomal membrane (and all other cellular membranes) with Triton X-100, a punctate distribution was manifest in addition to the background labeling (Fig. 3 *F*). The ability to detect punctate labeling only after permeabilization of the peroxisomal membrane indicates that AGT-pri (and AGT$^{\alpha}$) are imported into the peroxisomal interior and not just attached to the exterior of the organelle.

To ascertain whether the Gly170→Arg mutation interfered with the efficiency of AGT peroxisomal import,

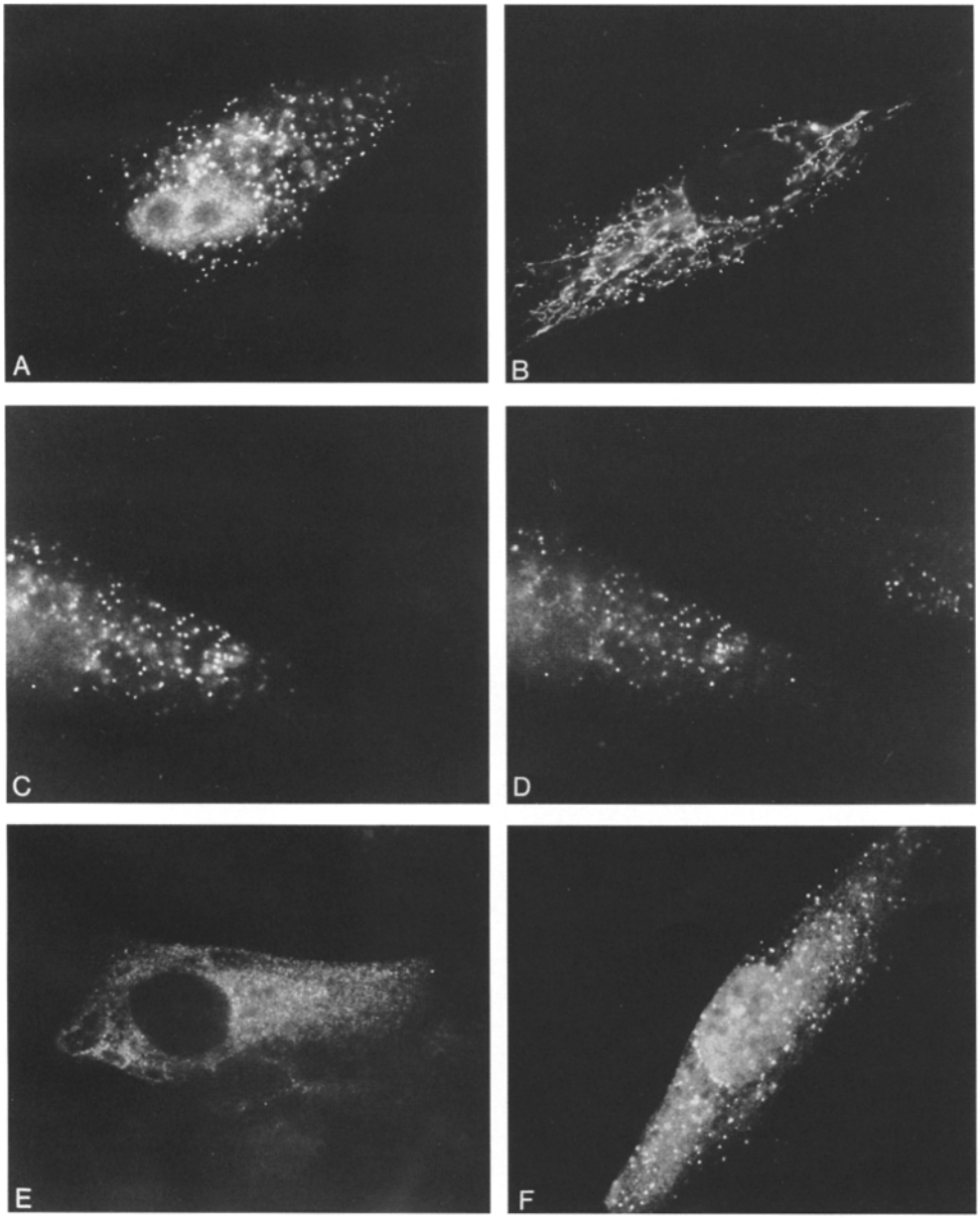

Figure 3. Intracellular localization of various artificial derivatives of AGT in normal human fibroblasts. (*A*) AGT-lgi; (*B*) AGT-lri; (*C* and *D*) double labeling of AGT-pri (*C*) and peroxisomal thiolase (*D*); (*E*) AGT-pri in cells permeabilized with 25 μg/ml digitonin; (*F*) AGT-pri in cells permeabilized with digitonin plus Triton X-100.

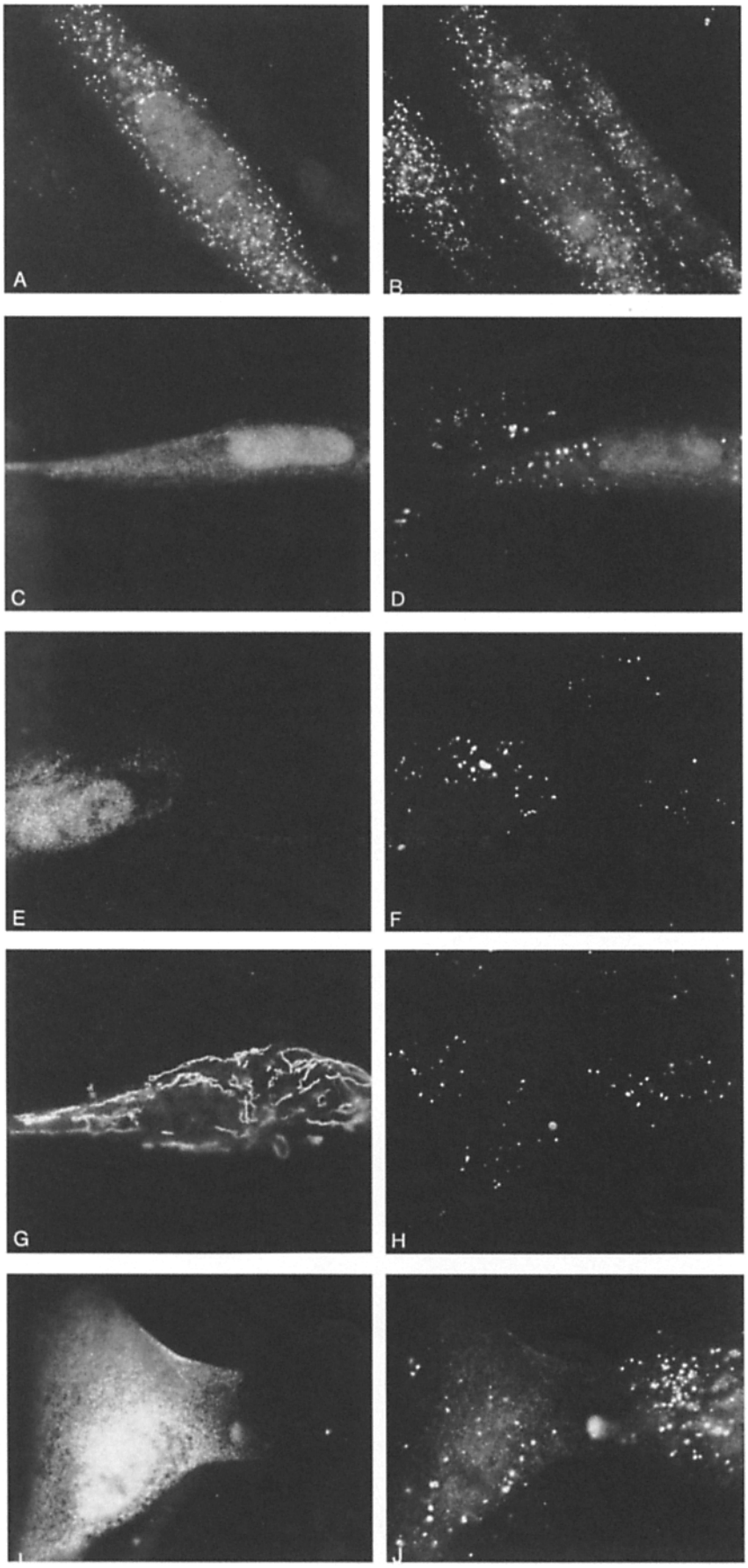

Figure 4. Intracellular localization of various AGTs in human fibroblasts deficient in either PTS1 or PTS2-mediated import. Double labeling of AGT (*A*) and peroxisomal catalase (*B*) in PTS2$^-$ cells. Double labeling of AGT$^\alpha$ (*C*), AGT$^\beta$ (*E*), AGT$^\gamma$ (*G*), and AGT-pri (*I*) and peroxisomal thiolase (*D*, *F*, *H*, and *J*, respectively) in PTS1$^-$ cells.

rather than inhibiting it completely, AGT localization was determined 2.5 h after the microinjection of pAGT-pri (and pAGT$^{\alpha}$) and compared with that found after the normal incubation time of 18 h (see Materials and Methods). Although much more diffuse cytosolic labeling was noticeable after this short period of time, there was no obvious difference in the relative proportion of punctate labeling between AGT-pri and AGT$^{\alpha}$ (data not shown), indicating that the Gly170→Arg mutation did not significantly decrease the efficiency of AGT peroxisomal import.

Identification of the Peroxisomal Import Pathway for AGT

To determine the specific peroxisomal import pathway used by AGT, normal and mutant forms of the protein were expressed in fibroblasts in which import via either the PTS1 or PTS2 pathways is defective (Fig. 4). Expression of pAGT$^{\alpha}$ in PTS2^{-} fibroblasts, which fail to import thiolase (24), gave rise to a punctate pattern of labeling that colocalized with peroxisomal catalase (Fig, 4, *A* and *B*). This indicates that the peroxisomal import of AGT$^{\alpha}$ does not involve the component of the thiolase (PTS2) import pathway that is deficient in these cells. On the other hand, when expressed in PTS1^{-} fibroblasts, which fail to import firefly luciferase and other PTS1-containing proteins into peroxisomes (24), neither AGT$^{\alpha}$ nor AGT$^{\beta}$ were localized in a particulate fashion but were instead evenly dispersed throughout the cytosol (Fig. 4, *C–F*). This finding suggests that the peroxisomal import of AGT$^{\alpha}$ and AGT$^{\beta}$ does involve the component of the PTS1 import pathway that is deficient in these cells. The cytosolic compartmentalization of AGT$^{\alpha}$ and AGT$^{\beta}$ in PTS1^{-} fibroblasts is very similar to that of endogenously expressed AGT in ZS liver, except that in the case of AGT$^{\beta}$ a small proportion was also localized in the mitochondria in ZS cells (see Table III) (9).

As expected, AGT$^{\gamma}$, when expressed in PTS1^{-} cells, was localized solely within the mitochondria (Fig. 4, *G* and *H*). However, when AGT-pri was expressed in such cells, the distribution was diffuse with no indication of mitochondrial labeling (Fig. 4, *I* and *J*). This observation confirms previous results obtained from isolated mitochondrial in vitro import studies (35) that the Gly170→Arg mutation found in some PH1 patients does not on its own directly affect mitochondrial import even in the absence of an effective peroxisomal import machinery.

Characterization of the Peroxisomal Targeting Sequence of AGT

After the observation that the Gly170→Arg mutation did not inhibit AGT peroxisomal targeting, and therefore could not contribute to the peroxisome-to-mitochondrion mistargeting phenomenon by interfering with any putative "internal" PTSs (see reference 4), and the observation that AGT was probably imported into peroxisomes via the PTS1 pathway, the role of the COOH terminus of AGT in peroxisomal targeting and import was investigated. When the COOH-terminal tripeptide KKL was deleted from normal human AGTs (i.e., AGT$^{\alpha}$-Δ1 and AGT$^{\beta}$-Δ1), peroxisomal import in normal fibroblasts was totally abolished, as it was when the KKL of AGT$^{\alpha}$ was replaced by SEL, DEL or LLL (Fig. 5, *A–D*). However, when the KKL of AGT$^{\alpha}$ was replaced by the COOH-terminal tripeptides found in the AGT of other mammalian species (i.e., SQL and NKL), or the prototypical PTS1 from firefly luciferase (i.e., SKL), or even SSL, peroxisomal targeting

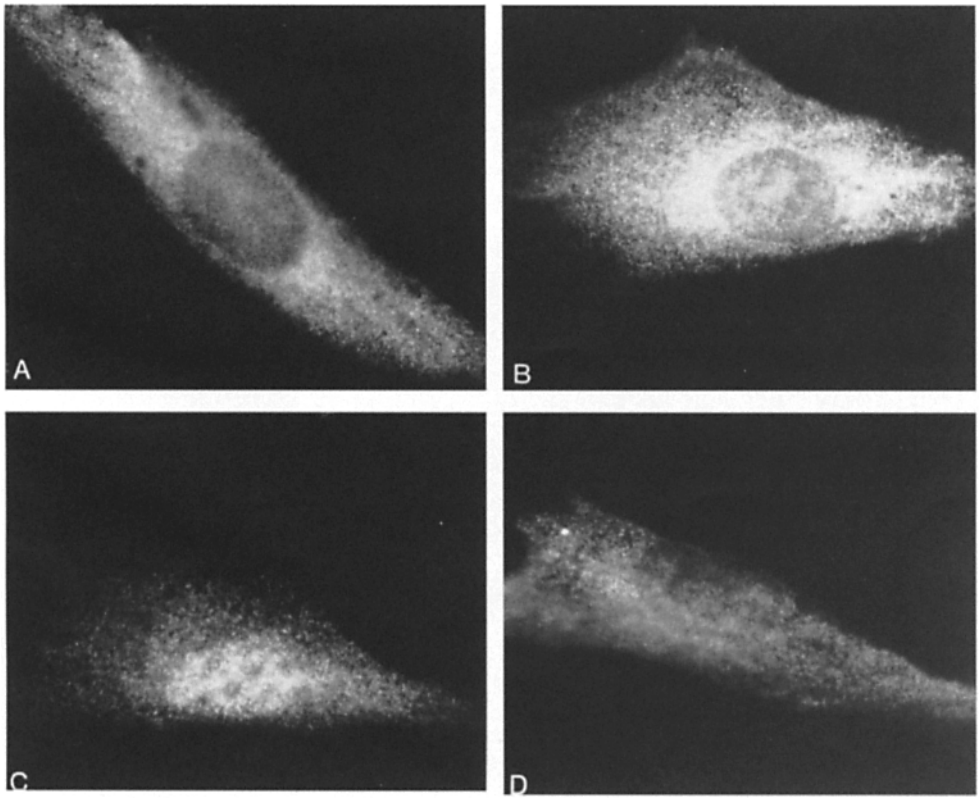

Figure 5. Intracellular localization of various COOH-terminally mutated derivatives of AGT that fail to be imported into peroxisomes in normal human fibroblasts. (*A*) AGT-Δ1; (*B*) AGT-SEL; (*C*) AGT-DEL; (*D*) AGT-LLL.

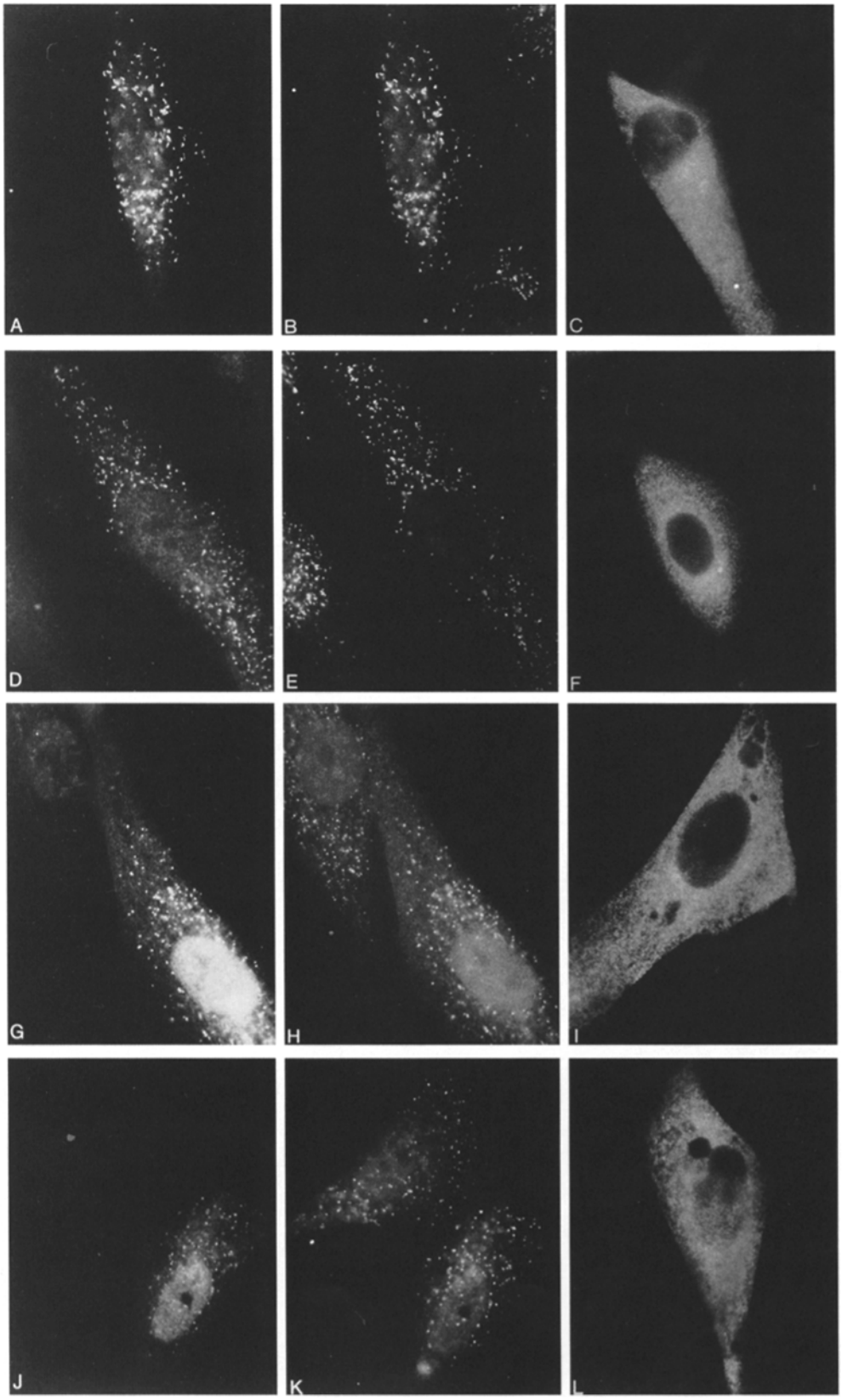

Figure 6. Intracellular localization of various COOH-terminally mutated derivatives of AGT that are imported into peroxisomes in normal fibroblasts. Double labeling of AGT (*left column*) and peroxisomal thiolase (*center column*). Panels on the right show labeling pattern when cells expressing the AGT derivatives are permeabilized with 25 μg/ml digitonin. (*A* and *C*) AGT-SQL; (*D* and *F*) AGT-NKL; (*G* and *I*) AGT-SKL; (*J* and *L*) AGT-SSL. As has been found previously (24), nuclear fluorescence is sometimes observed after intranuclear microinjection of expression plasmids (see *G* and *I*). This finding is idiosyncratic and currently defies explanation. However, in the present study at least, nuclear fluorescence was highly variable and unrelated to any particular construct.

and import was maintained (Fig. 6, *A–L*). In all cases, selective permeabilization using digitonin demonstrated that punctate labeling was due to import into the peroxisomal matrix and not adherence to the exterior of the organelle (Fig. 6, *C, F, I, L*). Mitochondrial labeling was not detected with any of the COOH-terminal mutants, even when AGT^{β}-Δ1 (or AGT^{α}-Δ1) was expressed in $PTS1^{-}$ cells (data not shown). A summary of the results of the in-

tracellular compartmentalization of the various COOH-terminally mutated as well as other AGT derivatives is shown in Table III.

These results are compatible with the COOH-terminal tripeptides of human, marmoset, rabbit, rat, and cat AGTs all being PTS1s. However, even though KKL is clearly necessary for the correct intracellular compartmentation of AGT, it appears to be unable to direct the targeting and import of another peroxisomal protein (i.e., firefly luciferase). Although unmodified firefly luciferase has already been shown to be targeted and imported into the peroxisomes of normal fibroblasts (24), substitution of the COOH-terminal SKL by KKL in the present study abolished targeting (Fig. 7). A similar result has been found previously using transfected monkey CV-1 cells (15). In addition, although the prototypical PTS1, SKL, was able to target the reporter protein CAT to the peroxisomes in the present system, KKL was unable to do so (Fig. 8).

In an attempt to determine whether any part of the AGT polypeptide contiguous with the COOH-terminal KKL might play a role in its peroxisomal targeting, two constructs (AGT-Δ2 and AGT-Δ3) were made in which the 10 or 44 amino acids, respectively, immediately upstream of the KKL were deleted. These constructs failed to be targeted to peroxisomes (Fig. 9, *A–D*), suggesting either that the PTS1 of AGT extends beyond its COOH-terminal tripeptide, or that the regions deleted provide at least part of the structural context within which KKL is able operate as a PTS1. However, despite the apparent necessity of these internal sequences for the peroxisomal targeting of AGT, neither the COOH-terminal 13 or 47 amino acids (including the KKL) of AGT were able to target the CAT-fusions CAT+AGT13 and CAT+AGT47 to peroxisomes (Fig. 9, *E–H*). It is very unlikely that the failure of CAT+AGT47 to target to peroxisomes is due to any structural imcompatibility between the CAT and AGT polypeptide sequences that might lead to aggregation etc., as a similar construct (CAT+AGT47-SKL) in which the COOH-terminal KKL was replaced by SKL was imported into peroxisomes (data not shown).

Discussion

The observation that the peroxisomal targeting of AGT^{α} and AGT^{β} is completely abolished when expressed in $PTS1^{-}$ fibroblasts, but is completely normal in $PTS2^{-}$ fibroblasts, inevitably leads to the conclusion that AGT is targeted and imported into peroxisomes by way of at least one component of the PTS1 import machinery. Complementation analysis has shown that a single gene defect is responsible for peroxisomal dysfunction in the AAL85AD ($PTS1^{-}$) cell line (2). In addition, a mutation has recently been identified in the putative PTS1-receptor gene in this cell line (13) (described as cell line PBD018 in the latter publication). Therefore, it is likely that AGT is imported into peroxisomes by way of the PTS1 receptor, and, consequently, it is equally likely that the PTS of AGT is a PTS1.

The mammalian PTS1, as currently defined, consists of a simple tripeptide based on the SKL motif that is only functional when placed at the COOH terminus. Even a single amino acid addition (15) or amidation of the α-carboxyl group (22) can abolish targeting. Internal SKLs or similar motifs that have from time to time been speculated to be PTSs (25) have never been proven to be so. Targeting sequences, including PTSs, are usually defined as those sequences that are both necessary and sufficient to direct the targeting of polypeptides to a particular organelle, and the prototypical PTS1 (i.e., SKL) certainly fulfils these general requirements (14). However, the data presented in this paper on the targeting of AGT suggest that either the general definition of targeting sequences, at least as applied to PTS1s, is inadequate or that the currently recognized description of the mammalian PTS1 is incomplete.

The finding that the import of both AGT^{α} and AGT^{β} into peroxisomes of normal human fibroblasts is completely abolished when the COOH-terminal KKL is deleted is indicative of the necessity of this sequence for the protein's correct intracellular compartmentalization. However, previous studies have already shown that KKL is not sufficient to target firefly luciferase either to peroxisomes of monkey kidney CV-1 cells (15) or to glycosomes of *Trypanosoma brucei* (38), and in the present study KKL has been shown to be insufficient to target firefly luciferase or CAT to peroxisomes in human fibroblasts. Therefore, the COOH-terminal KKL of human AGT, which has a 2/3 match with the prototypical PTS1 SKL, would appear to be able to fulfil only one of the general requirements of a targeting sequence (i.e., it is necessary).

There are at least two possible explanations for these apparently contradictory findings. The first is that KKL might be able to act as a PTS1 only within a particular structural context, the role of which might be concerned with the presentation of the PTS1, rather than being part of the PTS1 itself. The efficiency with which the PTS1 is

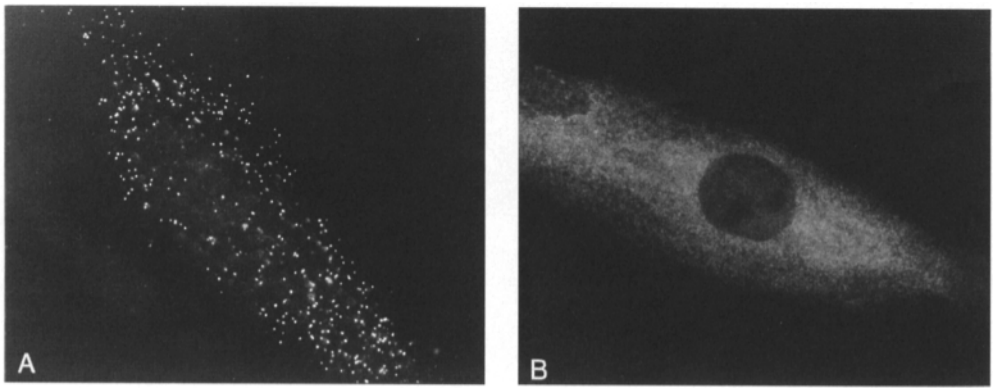

Figure 7. Intracellular localization of firefly luciferase-SKL (*A*) and luciferase-KKL (*B*) in normal human fibroblasts.

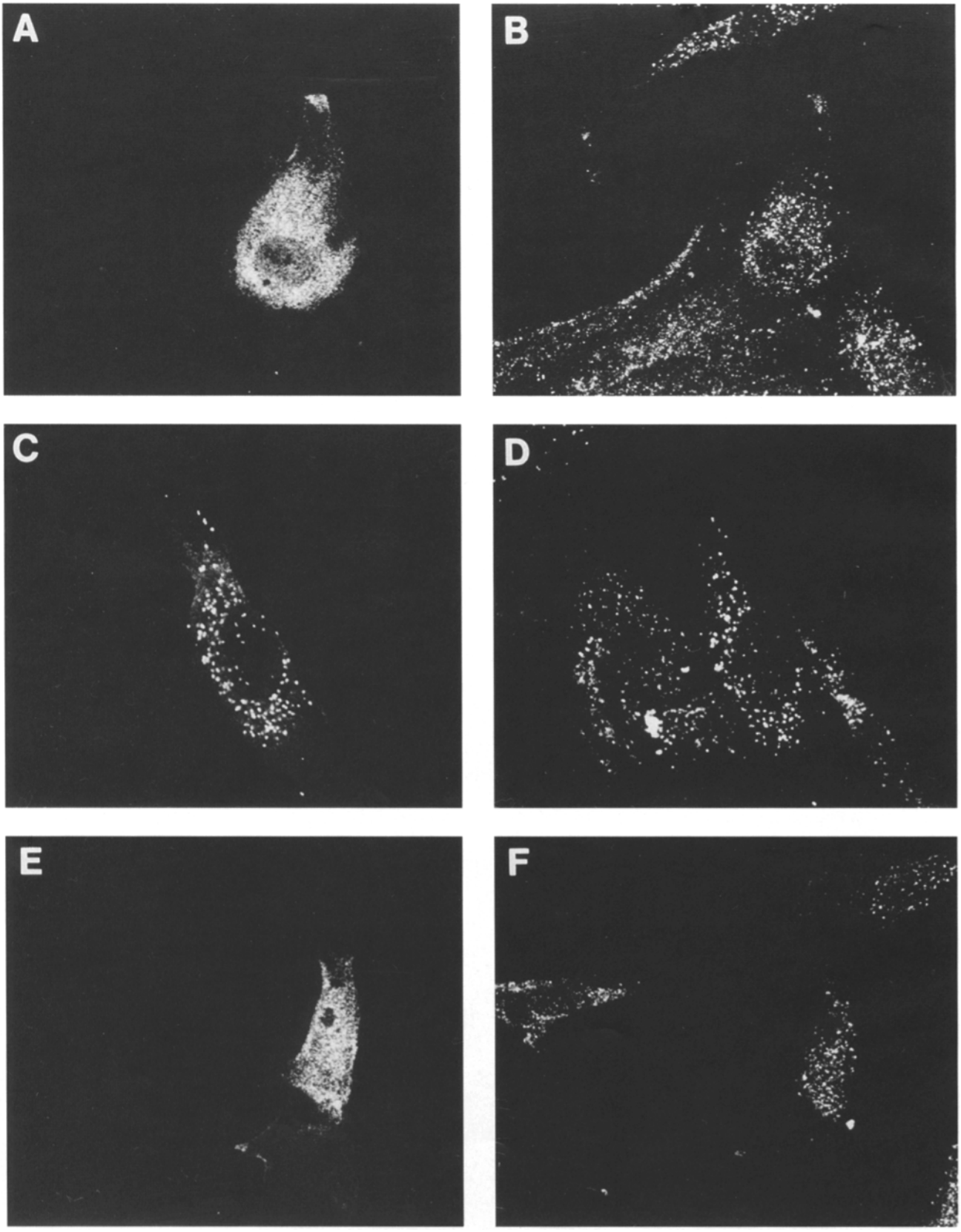

Figure 8. Intracellular localization of CAT and various COOH-terminal CAT fusions in normal human fibroblasts. Double labeling of CAT (*A*), CAT-SKL (*C*), CAT-KKL (*E*), and catalase (*B*, *D*, and *E*, respectively), immunofluorescence being observed by confocal laser-scanning microscopy.

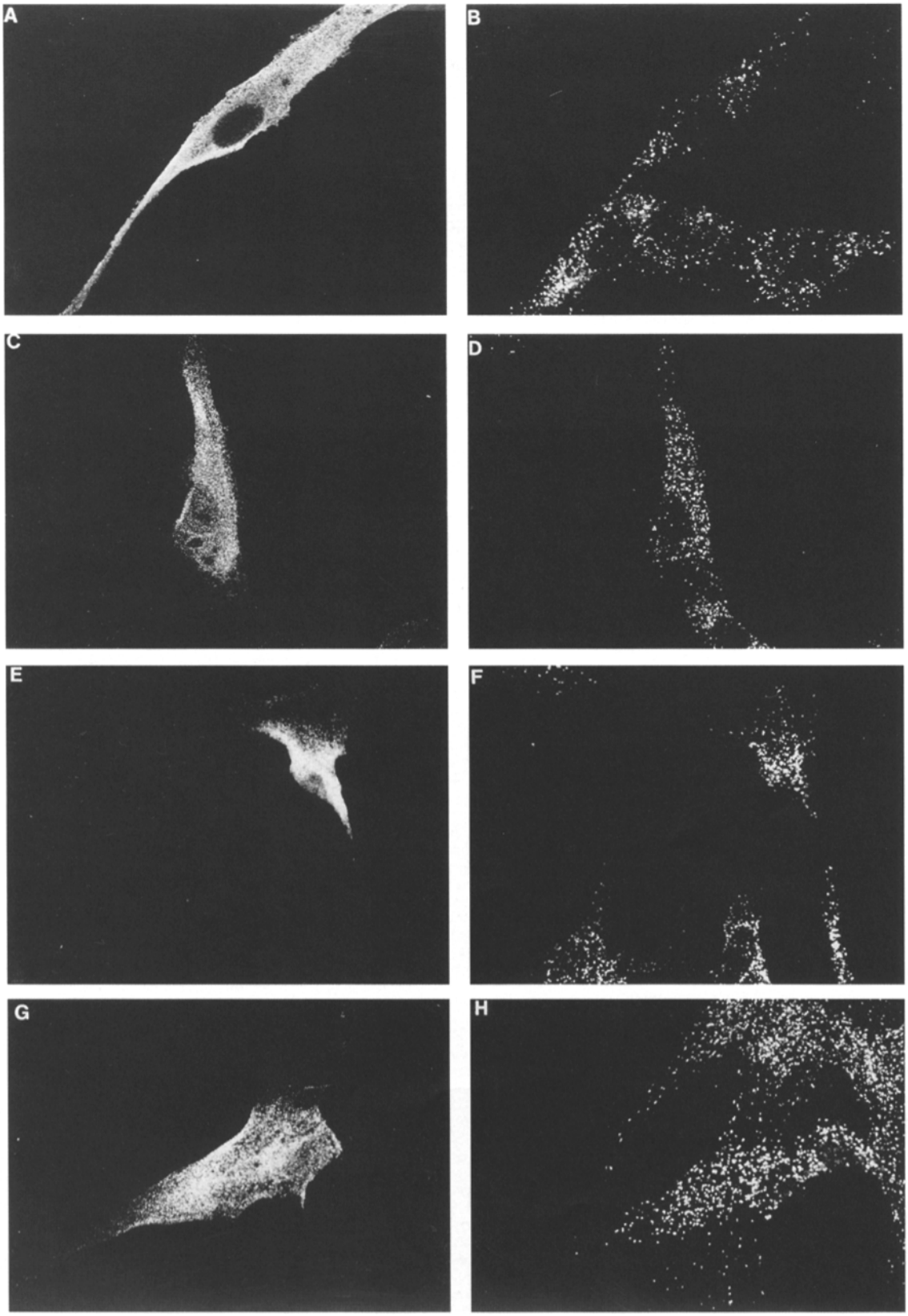

Figure 9. Intracellular localization of AGT internal deletions and CAT-AGT fusions in normal human fibroblasts. Double labeling of AGT internal deletions AGTα-Δ2 (*A*), AGTα-Δ3 (*C*), CAT-AGT fusions CAT+AGT13 (*E*), CAT+AGT47 (*G*), and catalase (*B*, *D*, *F*, and *H*, respectively). The CAT-AGT fusions were detected using antibodies against CAT and not AGT.

presented to the PTS1 receptor is likely to be dependent on many factors, including polypeptide folding and/or oligomerization. Why the presentation of KKL should require a different context to that required by SKL is unknown. It is also puzzling that, although the context within which the PTS1 of AGT is required to operate is very specific (i.e., AGT provides the context but FFL and CAT do not), the PTS1 itself is very degenerate. This clearly has major implications for the targeting of other peroxisomal proteins that do not appear to possess the minimum consensus PTS1, as currently defined. If AGT, and possibly other peroxisomal proteins as well, do possess enabling sequences not directly involved in targeting, then the classical definition of a PTS as being both "necessary and sufficient" would appear to be no longer adequate. A perfectly genuine PTS1 might be able to target only one, or a limited number of proteins to the peroxisomes. This might even apply to the prototypical PTS1, as previous studies have shown that in *Saccharomyces cerevisiae* a COOH-terminal SKL can direct the peroxisomal import of firefly luciferase, whereas it is unable to do so for dihydrofolate reductase (12). As far as AGT is concerned, it is not yet known what part of the polypeptide provides the correct context, except that the sequence immediately adjacent to the COOH-terminal KKL (i.e., the last 47 amino acids) is unable to do so.

A survey of the literature reveals a number of instances, especially in heterologous import systems, where COOH-terminal sequences in peroxisomal proteins have been shown to be necessary but not sufficient (1, 12), and some where they have been shown to be sufficient but not necessary (19). In the present study, AGT has been expressed in an homologous system, in so far as both polypeptide and cell line were human in origin. This situation is frequently not possible in peroxisomal import studies due to the interference from endogenous gene expression. In the present case, advantage has been made of the fact that AGT is expressed in a cell-specific manner (i.e., although AGT is expressed at high levels in human hepatocytes, endogenous expression in human fibroblasts is undetectable). For studies into peroxisomal protein targeting, firefly luciferase and other reporter polypeptides, such as CAT, are almost always expressed or otherwise introduced into heterologous systems (i.e., into cells from genera, classes, phyla, or even kingdoms different to those from which the polypeptide originated). Although this approach has shown that many aspects of the peroxisomal import pathway are evolutionarily conserved (16, 18), extrapolations between different heterologous systems can be problematic.

A second possible explanation of our findings, with respect to the peroxisomal targeting of AGT, is that the current definition of the PTS1 is incomplete. The PTS1 in some peroxisomal proteins might extend beyond the COOH-terminal tripeptide, possibly including noncontiguous sequences. If the PTS1 is different in different proteins, then each protein might be expected to interact with the PTS1 receptor differently. For example, the putative non–COOH-terminal component of the PTS1 of AGT might interact with the PTS1 receptor or an accessory protein in a way that allosterically modifies the interaction of the COOH-terminal component (i.e., KKL) with the receptor. Such a dual interaction could also modify the allowable degeneracy of the COOH-terminal part of the PTS1 to include sequences as dissimilar as KKL, NKL, SQL, SKL, and SSL, as found in the present study. On the other hand, classical PTS1s (i.e., SKL etc. [15, 41]) might bind to the PTS1 receptor with such high affinity that additional sequences outside the COOH-terminal tripeptide are not necessary.

The role of the Gly170→Arg mutation in the AGT of PH1 patients manifesting the peroxisome-to-mitochondrion AGT mistargeting phenotype remains an enigma (6, 34). Results obtained in the present study exclude the possibility that it potentiates the functional efficiency of the MTS generated by the Pro11→Leu polymorphism by interfering with AGT peroxisomal targeting or import. A molecular explanation of its remarkable in vivo-specific facilitating action (34, 35) will have to await the outcome of further study.

We would like to thank Dr. E. Middelkoop for introducing us to the technique of microinjection.

Received for publication 12 December 1994 and in revised form 22 June 1995.

References

1. Aitchison, J. D., W. W. Murray, and R. A. Rachubinski. 1991. The carboxyl-terminal tripeptide Ala-Lys-Ile is essential for targeting *Candida tropicalis* trifunctional enzyme to yeast peroxisomes. *J. Biol. Chem.* 266: 23197–23203.
2. Brul, S., A. Westerveld, A. Strijland, R. J. Wanders, A. W. Schram, H. S. Heymans, R. B. Schutgens, H. van den Bosch, and J. M. Tager. 1988. Genetic heterogeneity in the cerebrohepatorenal (Zellweger) syndrome and other inherited disorders with a generalized impairment of peroxisomal functions. A study using complementation analysis. *J. Clin. Invest.* 81: 1710–1715.
3. Cooper, P. J., C. J. Danpure, P. J. Wise, and K. M. Guttridge. 1988. Immunocytochemical localization of human hepatic alanine:glyoxylate aminotransferase in control subjects and patients with primary hyperoxaluria type 1. *J. Histochem. Cytochem.* 36:1285–1294.
4. Danpure, C. J. 1993. Primary hyperoxaluria type 1 and peroxisome-to-mitochondrion mistargeting of alanine:glyoxylate aminotransferase. *Biochimie (Paris).* 75:309–315.
5. Danpure, C. J., and P. E. Purdue. 1995. Primary hyperoxaluria. *In* The Metabolic and Molecular Bases of Inherited Disease. C. R. Scriver, A. L. Beaudet, W. S. Sly, and D. Valle, editors. McGraw-Hill, NY. 2385–2424.
6. Danpure, C. J., P. J. Cooper, P. J. Wise, and P. R. Jennings. 1989. An enzyme trafficking defect in two patients with primary hyperoxaluria type 1: peroxisomal alanine/glyoxylate aminotransferase rerouted to mitochondria. *J. Cell Biol.* 108:1345–1352.
7. Danpure, C. J., K. M. Guttridge, P. Fryer, P. R. Jennings, J. Allsop, and P. E. Purdue. 1990. Subcellular distribution of hepatic alanine:glyoxylate aminotransferase in various mammalian species. *J. Cell Sci.* 97:669–678.
8. Danpure, C. J., P. E. Purdue, P. Fryer, S. Griffiths, J. Allsop, M. J. Lumb, K. M. Guttridge, P. R. Jennings, J. I. Scheinman, S. M. Mauer, and N. O. Davidson. 1993. Enzymological and mutational analysis of a complex primary hyperoxaluria type 1 phenotype involving alanine:glyoxylate aminotransferase peroxisome-to-mitochondrion mistargeting and intraperoxisomal aggregation. *Am. J. Hum. Genet.* 53:417–432.
9. Danpure, C. J., P. Fryer, S. Griffiths, K. M. Guttridge, P. R. Jennings, J. Allsop, A. B. Moser, S. Naidu, H. W. Moser, M. MacCollin, and D. C. DeVivo. 1994. Cytosolic compartmentalization of hepatic alanine:glyoxylate aminotransferase in patients with aberrant peroxisomal biogenesis and its effect on oxalate metabolism. *J. Inher. Metab. Dis.* 17:27–40.
10. Danpure, C. J., P. Fryer, P. R. Jennings, J. Allsop, S. Griffiths, and A. Cunningham. 1994. Evolution of alanine:glyoxylate aminotransferase 1 peroxisomal and mitochondrial targeting. A survey of it subcellular distribution in the livers of various representatives of the classes Mammalia, Aves and Amphibia. *Eur. J. Cell Biol.* 64:295–313.
11. de Hoop, M. J., and G. Ab. 1992. Import of proteins into peroxisomes and other microbodies. *Biochem. J.* 286:657–669.
12. Distel, B., S. J. Gould, T. Voorn Brouwer, M. van der Berg, H. F. Tabak, and S. Subramani. 1992. The carboxyl-terminal tripeptide serine-lysine-leucine of firefly luciferase is necessary but not sufficient for peroxisomal import in yeast. *New Biol.* 4:157–165.
13. Dodt, G., N. Braverman, C. Wong, A. Moser, H. W. Moser, P. Watkins, D.

Valle, and S. J. Gould. 1995. Mutations in the PTS1 receptor gene, PXR1, define complementation group 2 of the peroxisome biogenesis disorders. *Nature Genet.* 9:115–125.
14. Gould, S. G., G. A. Keller, and S. Subramani. 1987. Identification of a peroxisomal targeting signal at the carboxy terminus of firefly luciferase. *J. Cell Biol.* 105:2923–2931.
15. Gould, S. J., G. A. Keller, N. Hosken, J. Wilkinson, and S. Subramani. 1989. A conserved tripeptide sorts proteins to peroxisomes. *J. Cell Biol.* 108:1657–1664.
16. Gould, S. J., G. A. Keller, M. Schneider, S. H. Howell, L. J. Garrard, J. M. Goodman, B. Distel, H. Tabak, and S. Subramani. 1990. Peroxisomal protein import is conserved between yeast, plants, insects and mammals. *EMBO J.* 9:85–90.
17. Heikoop, J. C., M. Van Den Berg, A. Strijland, P. J. Weijers, R. B. Schutgens, W. W. Just, R. J. Wanders, and J. M. Tager. 1991. Peroxisomes of normal morphology but deficient in 3-oxoacyl-CoA thiolase in rhizomelic chondrodysplasia punctata fibroblasts. *Biochim. Biophys. Acta.* 1097:62–70.
18. Keller, G. A., S. Gould, M. Deluca, and S. Subramani. 1987. Firefly luciferase is targeted to peroxisomes in mammalian cells. *Proc. Natl. Acad. Sci. USA.* 84:3264–3268.
19. Kragler, F., A. Langeder, J. Raupachova, M. Binder, and A. Hartig. 1993. Two independent peroxisomal targeting signals in catalase A of *Saccharomyces cerevisiae*. *J. Cell Biol.* 120:665–673.
20. Luckow, B., and G. Schutz. 1987. CAT constructions with multiple unique restriction sites for the functional analysis of eukaryotic promoters and regulatory elements. *Nucl. Acids Res.* 15:5490.
21. Lumb, M. J., P. E. Purdue, and C. J. Danpure. 1994. Molecular evolution of alanine/glyoxylate aminotransferase 1 intracellular targeting: analysis of the feline gene. *Eur. J. Biochem.* 221:53–62.
22. Miura, S., I. Kasuya Arai, H. Mori, S. Miyazawa, T. Osumi, T. Hashimoto, and Y. Fujiki. 1992. Carboxyl-terminal consensus Ser-Lys-Leu-related tripeptide of peroxisomal proteins functions in vitro as a minimal peroxisome-targeting signal. *J. Biol. Chem.* 267:14405–14411.
23. Mori, M., T. Oda, K. Nishiyama, T. Serikawa, J. Yamada, and A. Ichiyama. 1992. A single serine:pyruvate aminotransferase gene on rat chromosome 9q34-q36. *Genomics.* 13:686–689.
24. Motley, A., E. Hettema, B. Distel, and H. Tabak. 1994. Differential protein import deficiencies in human peroxisome assembly disorders. *J. Cell Biol.* 125:755–767.
25. Nishiyama, K., G. Berstein, T. Oda, and A. Ichiyama. 1990. Cloning and nucleotide sequence of cDNA encoding human liver serine-pyruvate aminotransferase. *Eur. J. Biochem.* 194:9–18.
26. Noguchi, T., Y. Minatogawa, Y. Takada, E. Okuno, and R. Kido. 1978. Subcellular distribution of pyruvate (glyoxylate) aminotransferases in rat liver. *Biochem. J.* 170:173–175.
27. Noguchi, T., and Y. Takada. 1979. Peroxisomal localization of alanine: glyoxylate aminotransferase in human liver. *Arch. Biochem. Biophys.* 196: 645–647.
28. Noguchi, T., Y. Takada, and Y. Oota. 1979. Intraperoxisomal and intramitochondrial localization, and assay of pyruvate (glyoxylate) aminotransferase from rat liver. *Hoppe-Seylers. Z. Physiol. Chem.* 360:919–927.
29. Oda, T., T. Funai, and A. Ichiyama. 1990. Generation from a single gene of two mRNAs that encode the mitochondrial and peroxisomal serine:pyruvate aminotransferase of rat liver. *J. Biol. Chem.* 265:7513–7519.
30. Oda, T., H. Miyajima, Y. Suzuki, and A. Ichiyama. 1987. Nucleotide sequence of the cDNA encoding the precursor for mitochondrial serine: pyruvate aminotransferase of rat liver. *Eur. J. Biochem.* 168:537–542.
31. Okuno, E., Y. Minatogawa, J. Nakanishi, M. Nakamura, N. Kamoda, M. Makino, and R. Kido. 1979. The subcellular distribution of alanine-glyoxylate aminotransferase and serine-pyruvate aminotransferase in dog liver. *Biochem. J.* 182:877–879.
32. Osumi, T., T. Tsukamoto, S. Hata, S. Yokota, S. Miura, Y. Fujiki, M. Hijikata, S. Miyazawa, and T. Hashimoto. 1991. Amino-terminal presequence of the precursor of peroxisomal 3-ketoacyl-CoA thiolase is a cleavable signal peptide for peroxisomal targeting. *Biochem. Biophys. Res. Commun.* 181:947–954.
33. Pelham, H. R., K. G. Hardwick, and M. J. Lewis. 1988. Sorting of soluble ER proteins in yeast. *EMBO J.* 7:1757–1762.
34. Purdue, P. E., Y. Takada, and C. J. Danpure. 1990. Identification of mutations associated with peroxisome-to-mitochondrion mistargeting of alanine/glyoxylate aminotransferase in primary hyperoxaluria type 1. *J. Cell Biol.* 111:2341–2351.
35. Purdue, P. E., J. Allsop, G. Isaya, L. E. Rosenberg, and C. J. Danpure. 1991. Mistargeting of peroxisomal L-alanine:glyoxylate aminotransferase to mitochondria in primary hyperoxaluria patients depends upon activation of a cryptic mitochondrial targeting sequence by a point mutation. *Proc. Natl. Acad. Sci. USA.* 88:10900–10904.
36. Purdue, P. E., M. J. Lumb, M. Fox, G. Griffo, C. Hamon Benais, S. Povey, and C. J. Danpure. 1991. Characterization and chromosomal mapping of a genomic clone encoding human alanine:glyoxylate aminotransferase. *Genomics.* 10:34–42.
37. Purdue, P. E., M. J. Lumb, and C. J. Danpure. 1992. Molecular evolution of alanine:glyoxylate aminotransferase 1 intracellular targeting. Analysis of the marmoset and rabbit genes. *Eur. J. Biochem.* 207:757–766.
38. Sommer, J. M., Q. L. Cheng, G. A. Keller, and C. C. Wang. 1992. In vivo import of firefly luciferase into the glycosomes of *Trypanosoma brucei* and mutational analysis of the C-terminal targeting signal. *Mol. Biol. Cell.* 3:749–759.
39. Subramani, S. 1993. Protein import into peroxisomes and biogenesis of the organelle. *Annu. Rev. Cell Biol.* 9:445–478.
40. Swinkels, B. W., S. J. Gould, A. G. Bodnar, R. A. Rachubinski, and S. Subramani. 1991. A novel, cleavable peroxisomal targeting signal at the amino-terminus of the rat 3-ketoacyl-CoA thiolase. *EMBO J.* 10:3255–3262.
41. Swinkels, B. W., S. J. Gould, and S. Subramani. 1992. Targeting efficiencies of various permutations of the consensus C-terminal tripeptide peroxisomal targeting signal. *FEBS (Fed. Eur. Biochem. Soc.) Lett.* 305:133–136.
42. Uchida, C., T. Funai, T. Oda, K. Ohbayashi, and A. Ichiyama. 1994. Regulation by glucagon of serine: pyruvate/alanine: glyoxylate aminotransferase gene expression in cultured rat hepatocytes. *J. Biol. Chem.* 269: 8849–8856.
43. Wiemer, E. A., R. Ofman, E. Middelkoop, M. de Boer, R. J. Wanders, and J. M. Tager. 1992. Production and characterisation of monoclonal antibodies against native and disassembled human catalase. *J. Immunol. Methods.* 151:165–175.
44. Yokota, S., and T. Oda. 1984. Fine localization of serine:pyruvate aminotransferase in rat hepatocytes revealed by a post-embedding immunocytochemical technique. *Histochemistry.* 80:591–595.
45. Yokota, S., T. Oda, and A. Ichiyama. 1987. Immunocytochemical localization of serine: pyruvate aminotransferase in peroxisomes of the human liver parenchymal cells. *Histochemistry.* 87:601–606.